

KINETIC MONTE CARLO SIMULATION OF PULSE CU30NI BEAD ON PLATE

A. CHIOCCA*, F. SOULIE*, F. DESCHAUX-BEAUME*,
J. MITCHELL** and C. BORDREUIL*

**Université de Montpellier, Montpellier France*

***Sandia labs Albuquerque, United States*

DOI 10.3217/978-3-85125-615-4-09

ABSTRACT

The purpose of this paper is to show a modelling scheme to predict rapidly three dimensionnal grain structure. The modelling is based on a plane thermal finite element for the process coupled with a monte carlo simulation for grain structure. To demonstrate the interest of this type of modelling the simulations are done for a squared pulse mode and results are compared with experimental results (EBSD) done during the work of A.Chiocca. The originality of the paper is that predictions of grain structure are investigated with current and arc voltage evolving with time. Results show the interest of using monte carlo simulation.

Keywords: Monte carlo simulation, grain structure, Binary alloy

INTRODUCTION

The grain structure has an important impact on complex phenomena as hot cracking during welding [1]. The grain structure depends on thermal transfer induced by the process variables. Different modelling of grain structure evolution during solidification can be found in the literature. The two main modellings commonly encountered to predict grain structure are the cellular automaton (CA) [2] and kinetic monte carlo simulation [3]. The first one describes the physics of solidification but it is costly from the numerical point of view. The second one is fast and can then be implemented for an engineering point of view. Sandia Labs proposes an open source software ssparks [4] that can model efficiently grain structure during welding based on a potts model. In ssparks software, different applications are available and can treat three dimensional grain structures. Pulse welding is implemented in kinetic MC simulation (kMC). KMC has also the advantage to take into account grain growth in the heat affected zone that is quite difficult with CA. This last phenomenon can play an important role on epitaxial growth.

The purpose of this paper is to compare experimental results obtained during the PhD of A.Chiocca [5] and results carried out with ssparks program for complex process solidification conditions. Experiments are simple beads on CuNi plate with pulse current. Process thermal simulation is carried out and temperatures and weld pool size are compared

with experimental results. Then, melting isotherm based on the process simulation are integrated in the kMC simulation.

Based on EBSD maps, the experimental results seem to indicate an equiaxed grain structure in the whole bead. It is also demonstrated that grain size and shape depend on location inside the bead. Based on different kMC simulations, explanations about the different grain size would be attributed to the process or to the metallurgy. Results demonstrates that kMC opens nice perspectives from engineering point of view.

EXPERIMENTAL RESULTS

A. Chiocca [5] conducted solidification experiments on Cu30Ni plate with 1.6mm of thickness, 150mm of length and 70mm of width. TIG was used to create the melt pool in the middle of the plate. To investigate the link between the current intensity and solidification front behaviour, it was chosen to use squared pulsed current. The welding power source was set to have a peak current of 133A during 300ms and a low current of 29A during 500ms. The welding speed is 3.5mm/s. Different experimental observations were done during the process. The plate is moved in order to ease image acquisition. Images were synchronized with data acquisition (current evolution). A high speed camera with a microscopic lens was located to observe the solidification front during the pulse. In figure 1, images obtained by the device with microscopic lens are shown.

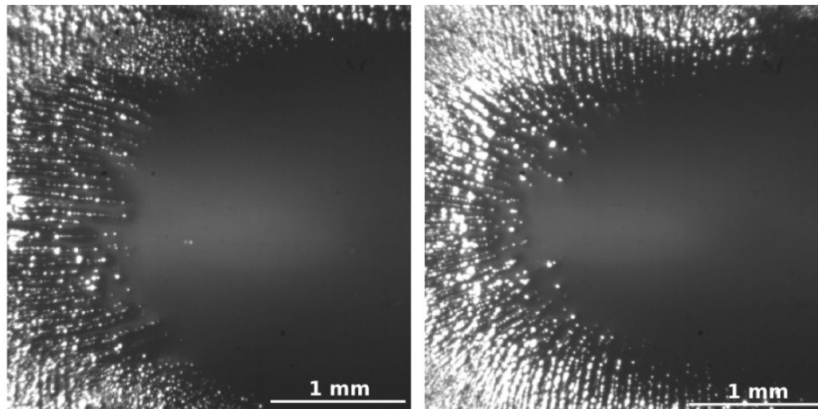


Fig. 1 Solidification front in the opposite side relative to the torch at the end of a low (right) and high current period (left).

Two cameras were located to observe the weld pool in the rear at the top and the bottom face of the plate. Basic image processing (canny) enables us to find the position at the rear of the weld pool in the frame of the camera. In order to have this position in a fixed frame in the plane of the plate, a calibration procedure was used. Based on the contour and with data acquisition synchronisation, it is possible to compare the evolution of the point at the rear as function of the current. Figure 2 shows the evolution of the position of the point at the rear of the weld pool and the evolution of the current. The curve of the position is noisy and it looks like a sine function. To investigate the position of the point, an interpolation was performed to identify the sine function with a least square method. The fit is good. The

position varies only from 0.5mm but this is for the point in the rear. In reality, there is a large evolution of the size of the weld pool. Cameras observations indicated that even at the end of the low current period there is still residual liquid at the center of the pool. In figure 2, the velocity of the front is derived from the fitted cosine function for the position and the experimental current shows a squared waveform. The front velocity is then approximated by a cosine function and shows a shift from the current that is due to the thermal transfer and in particular to thermal solidification time scale induced by the latent heat.

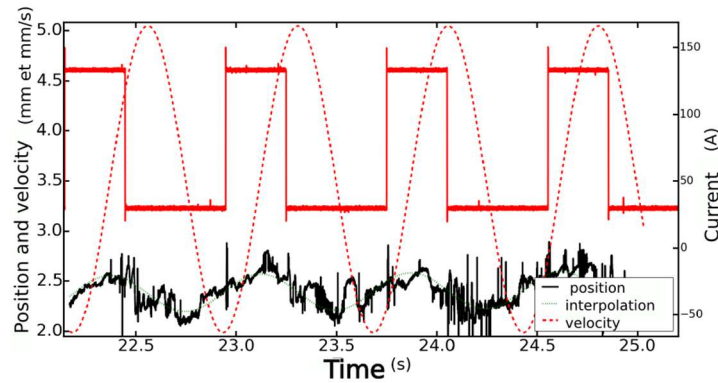


Fig. 2 Position of the point at the rear of the weld pool synchronised with current.

Figure 3 shows an EBSD map of a bead obtained with the present conditions. In figure 3, the assumed borders of the weld pool are drawn. The border is not easy to locate due to the large change in thermal transfer and due to possible grain growth in the heat affected zone. Compared to constant current weld bead with almost constant width, the width of the pool changes with the torch travelling. This will induce complex front velocity along the border of the weld pool that can modify considerably grain growth. The size of grain in the base material can be estimated with the EBSD measurement. For this plate, it is around 10 micrometers. In figure 3, the middle of the weld bead is shown. It seems that the weld pool is not symmetrical probably due to important fluid flow. The size of the grains can be estimated from the file given by the EBSD measurement. It seems that the grains are larger in the middle of the pool. The size of the grains is controlled by two phenomena. The first one corresponds to the growth of grains and the second one is due to nucleation. In liquid, nucleation can be due to inoculant (particles) or to dendritic arm broken due to active flow.

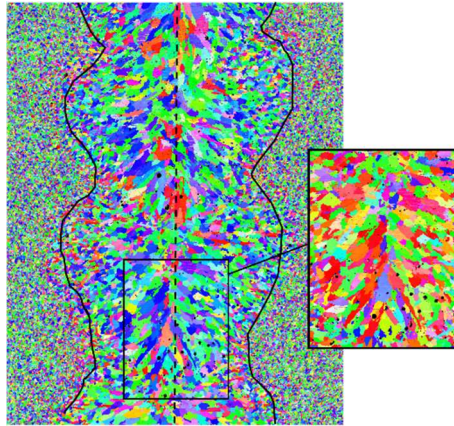


Fig. 3 EBSD map for the pulse test conditions at the top side of the plate. In black, assumed contour of the weld bead. Some porosities are visible (black disks) in the middle of the weld pool. The width of the weld pool is approximately 10mm. The image in the right has another color because it is another orientation.

To compare the grain structure inside the weld bead, regions of interest must be defined. Because the width of the weld pool changes with time, the grain structure is highly inhomogeneous with large grain size distribution. It is then complicated to investigate the relation between solidification conditions and grain size distribution. Nevertheless, to study this relationship, a region of interest will be located at the common width of the weld pool. The region of interest corresponds to a rectangle that will be translated along the welding direction. Inside this rectangle, the number of grains are counted. A filter was applied to delete all small grains from the analysis and it is then possible to plot the number of grain inside the window in function of the position in the bead. The number of grains inside this window tells us about the average grain size in function of the traveling distance. If the number of grains in the window are low, it means that the grains are large. This can be due to less nucleation site combined with important grain growth velocity. It has also to be noticed that the EBSD maps were carried out on the plane close to the torch and that three dimensional effect due to thermal transfer can be important.

Figure 4 shows the result. A 2.8 mm characteristic length corresponding to the distance between two current peaks can be measured. The location of small grains (low number of grains) corresponds to the location of the peak current. The difference between the low and high value for the number of grains is round 50%.

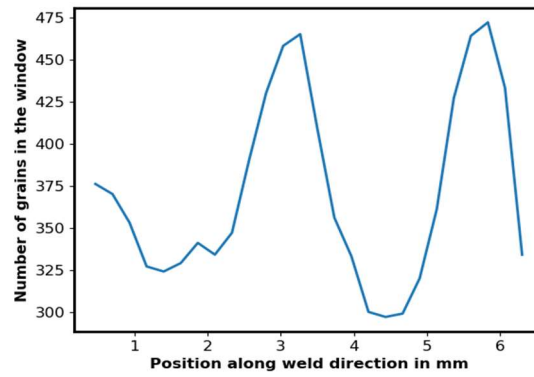


Fig. 4 Number of grains in function of the position along the weld direction computed with EBSD measurement.

PROCESS SIMULATION

In this part, the process simulation is explained. The purpose is to model the evolution of the solidification front in order to obtain the solidification front as function of time in order to feed the kinetic monte carlo simulation. The thermal transfers without taken into account fluid velocity are carried out. The different thermal properties of the Cu30Ni are given in table 1. With these properties, it is possible to estimate the characteristic solidification time due to the latent heat that is around 3s for the pool. It means that compared to the 1.2Hz of the pulsed current, latent heat has to be taken into account. In this purpose, an enthalpy formulation is modelled. This formulation integrates the phase change to compute the thermal fields.

Table 1 Thermal properties of Cu30Ni.

Property	Value and unit
Solidification interval	1472-1520K
Density	8940kg/m ³
Conductivity	60W/m.K
Capacity	600J/kg.K
Latent heat	2,75e5J/kg

Due to symmetry, only the half of the plate is modelled and to accelerate computation, we considered in plane conduction. Welding simulation follows classical theory. A surface gaussian flux (q) is used to model the heat input of the Gas tungsten arc in function of time t :

$$q = \frac{3 \eta U(t) I(t)}{\pi r_0^2} \exp\left(-3 \frac{(X - X_0)^2 + (Y - Y_0 - v_w t)^2}{r_0^2}\right) \quad (1)$$

where η is the efficiency of the process, $U(t)$, $I(t)$ are the arc voltage in function of time, r_0 is radius to model where the maximum of heat input entered the plate, X_0 and Y_0 are the coordinate of the start position of the torch and v_w is the welding speed assumed to be constant all along the process. The efficiency of the process is also assumed constant all along the process despite its possible fluctuations due to high convection during the peak current. Time increment is kept constant at 0.025s. More details about the modelling can be found in [5]. Based on melting isotherm, the evolution of the solidification front can be investigated as function of the time for several periods. Figure 5 shows the half width and length of the pool. The mean half width is around 2mm and the mean half length is 2.8mm. The two characteristics have an amplitude of 0.6mm. With the simulation, it is possible to know the position and the size of the melting isotherm with respect to time. The contour looks like an ellipsoid. The half width of the weld pool seems to be a sinusoid function while the half length of the weld pool seems to be more complex. For a first assumption, it is assumed to be fitted by a cosine function similar to the half width. Due to the difference of duration between the hot and cold period (0,3 vs 0,5 ms), it could be imagined a complex function to fit the evolution of the contour. In particular, it would be better to use a non symmetrical function. To investigate the possibility to use kMC simulation for complex solidification conditions, a cosine function is chosen for the radii of the ellipse that model geometrically the size of the melting isotherm. $a(t)$ and $b(t)$ are the two radii functions of time. The evolution of one radius is also shown in figure 5. If a mathematical function wants to fit the evolution of one radius of the ellipsoid, it can be chosen as:

$$a(t) = \left(\cos\left(\frac{2\pi}{\tau} t\right) \right) (a_{max} - a_{min}) + a_{min} \quad (2)$$

In figure 5, the result of the fit is excellent to approximate the evolution of the contour. By combining this evolution with the displacement of the center of the melting isotherm, it is possible to know the position of the solidification front. The center of the contours is assumed to move at a constant speed of 3.5mm/s.

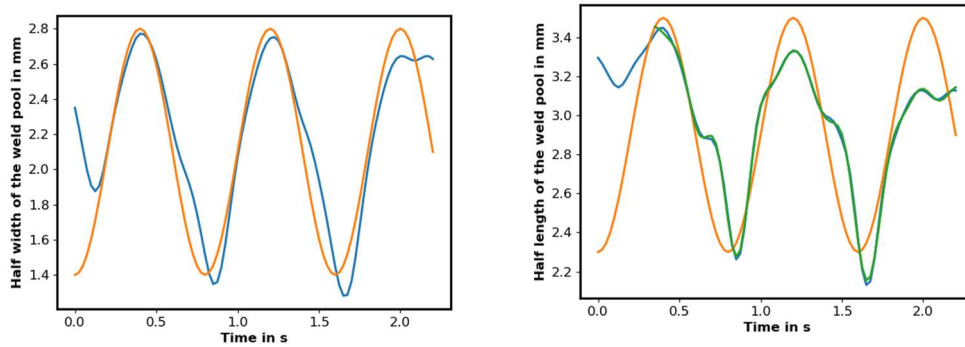


Fig. 5 Evolution of the fusion isotherm in function of the current for several periods The size of the weld pool is very similar to the experimental one.

KINETIC MONTE CARLO SIMULATION FOR GRAIN STRUCTURE PREDICTION

The kinetic monte carlo simulation tool used in this work is ssparks [4]. The base concept of the software is to minimize the grain boundary energy. The algorithm changes randomly spins in the neighbouring of a grain boundary site and looks if the change is energetically favorable or not with a probability function. Different applications are embedded in the code. In particular, the weld module is presented in [3]. In ssparks, pulse arc power is directly integrated in three dimensions. The weld pool is represented as an implicit function. The shape of the weld pool with the dissymetry between the top and the bottom is taken into account. The implicit function describing the one implemented in [3] looks like:

$$\rho(u, v) = V_0(v)P_0(u) + V_1(v)P_1(u) + V_2(v)P_2(u) \quad (3)$$

where u, v are two curvilinear abscissa and V and P are Bernstein polynomials and control points respectively. The two important features to model weld solidification with kinetic monte carlo simulation is the melting and the grain growth. The melting is modelled by assigning a random spin for point inside the weld pool. Grain growth is modelled by defining the grain boundary mobility function as:

$$M(T) = 1 - \frac{d(x)}{ha(t)} \quad (4)$$

where ha is a distance function depending on energy and $d(x)$ is the distance function from the weld pool. To take into account the evolution of energy during pulse current, ha function is defined in function of simulation time in a similar manner as the evolution for the radii (eq 2). During high current, the heat affected zone is larger. For the geometrical point of view, the workpiece is defined as a three dimensional structured grid also called a lattice. A cell of the grid is also called a site. The lattice has to model the width of the pool along x , the travelling in y direction and the thickness along z . Only a part embedding the weld pool is modelled in the geometry. The initial microstructure is computed by letting the grain growth occurs during a number of monte carlo steps (MCS). To have grains with a larger size, simulation are run with $2MCS$.

In the function describing the evolution of the weld pool, the time is also expressed as MCS and dimensions are expressed as function of a number of sites. A relationship exists between this time and real time, see [6] for more details. For given process conditions, it is assumed to be constant. For spatial synchronisation, a site represents a distance of 40 micrometers. This leads to a lattice of 400000 sites that is low cost to run and compare simulations. With these definitions, the weld pool dimensions a and b are to be defined in function of a number of sites and to model the evolution in figure 4 with time as MCS. The different parameters entering the monte carlo simulation are shown in table 2. The simulation time is expressed as monte carlo steps (MCS) as well as the welding velocity (scan rate).

Table 2 Parameters for kMC simulation

Parameter	Value and unit
Mean a radius	50 sites
Mean b radius	70 sites
Pulse period	32
Max Haz Distance	1
Scan rate	1.5.sites/MCS
Alpha coefficient for weld pool shape	0,.5
Beta coefficient	0.1

With these parameters, a first simulation is done. The results are shown in figure 6. The left hand side of figure 6 shows the initial grain structure obtained by letting the algorithm compute with a given initial number of seeds. The weld pool can be seen on the bottom of the domain. On right hand side, on the top of the figure, the weld pool was not gone out of the lattice. Despite the symmetry of the implicit function describing the solidification front, the result of grain structure is not symmetric due to the algorithm and due to the initial microstructure

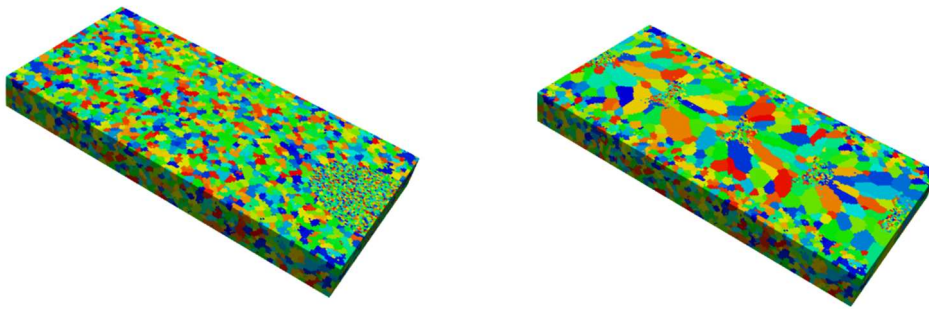


Fig. 6 Initial and final grain structure prediction after a pulse welding.

As for the experiment, large grains are visible and small grains are more located in the middle of the lattice. Figure 6 correspond to a top view of the plate. Due to the shape of the weld pool, the results are different on the bottom side. In fact, grain shapes on the bottom side look like more elongated denoting a large effect of the grain growth. The first result is to compare the overall distribution of the number of grains in a window as it was done for the experiment (see figure 4).

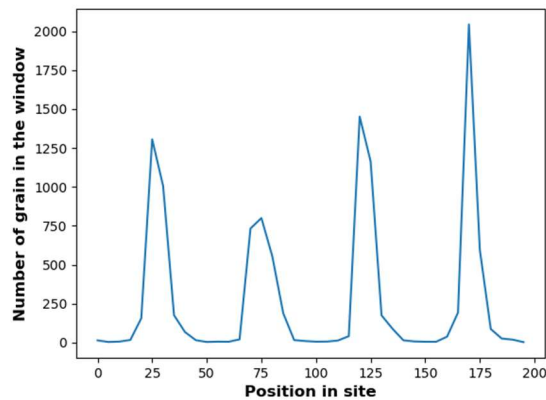


Fig. 7 Grain number in function of the direction of welding.

Figure 7 shows the distribution of grain number inside a cuboid with a side of 5 sites in length of welding, a side with the thickness of the plate and a side with the width of the weld pool. The period is equal to 70 sites that correspond to 2.4mm for the given velocity. Investigations indicates that small grains are generated at the end of the low current period. It is observed that large grains are then created during the rest of the low current period. One large grain is shown in figure 8.

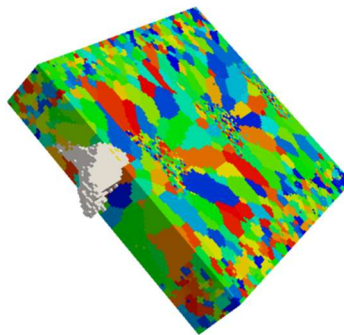


Fig. 8 A large grain inside the microstructure

In figure 8, the grain is extracted from the lattice by looking at the change of spins. The grain shown in figure 8 is large. It starts to grow from the bottom side of the plate and then grows to the top. It seems that most of the grains are columnar when investigating their three dimensionnal shapes and not equiaxed as can be indicated by observation of the top side.

CONCLUSION

The paper shows some comparison between experiments, process modelling and grain structure prediction. The base experiment is complex to model and lead to complex solidification conditions due to the squared current waveform. To predict the final grain structure in the bead, the most important is the weld pool border. Process simulation results with pulse mode show the complex evolution of the ellipsoid representing the weld pool border. The choice of implementing a sine function for radius is due to simplicity but more complex function can be implemented in order to have more precise evolution. The different model used in grain structure prediction (process and kMC simulation) are staggered and then uncoupled. This gives really fast computational time that to can be used for engineering purpose. Up to now, kMC does not take into account crystallographic orientation in the simulation. This orientation can be important to model some phenomena as hot cracking. Work in progress try to integrate crystallographic orientation in kMC simulation.

REFERENCES

- [1] C.BORDREUIL, A.NIEL. 'Modelling of hot cracking in welding with a cellular automaton combined with an intergranular fluid flow model', *COMP.MAT.SCI*, vol. **82** p.442 – 450,2014.
- [2] S.CHEN, G. GUILLEMOT G., C-A GANDIN., '*Three-dimensional cellular automaton-finite element modeling of solidification grain structures for arc-welding processes*', *Acta Materialia*, 115, 448-467, 2016
- [3] T.M.RODGERS, J.A.MICHELL, V.TIKARE 'A Monte Carlo model for 3D grain evolution during welding', *Modelling and Simulation in Materials Science and Engineering*, Volume 25, Number 6 , 2017
- [4] S.PLIMPTON, A.THOMPSON AND A.SLEPOY, SPPARKS, 2016. <http://spparks.sandia.gov>.
- [5] A.CHIocca : PhD Thesis, Université de Montpellier, 2016
- [6] Z.YANG S.SISTA, J.W.ELMER, T.DEBROY, 'Three dimensional monte carlo simulation of grain growth during GTA welding of titanium', *Acta Materialia*, Vol 48, p4813-4825, 2000
- [7] K.ICHIKAWA, A.NOGAMI,T.KOSEKI Y.FUKUDA, "Modelling of solidification and grain growth in steel welds", p189-207, *Mathematical modelling in welding 5*, Graz 2001.